

Modeling biases as norms for evaluating regional climate change

Z. Pan ^{*1}, J. H. Christensen², R. W. Arritt¹, W. J. Gutowski, Jr.^{1,3}, E. S. Takle^{1,3}, F. Otieno³

¹ Department of Agronomy, Iowa State University, USA

² Danish Meteorological Institute, Copenhagen, Denmark

³ Department of Geological and Atmospheric Sciences, Iowa State University, USA

Submitted to JGR special issue:

Advances in Regional Climate Modeling - ARCM

December 11, 1999

*Corresponding author address: Dr. Zaitao Pan, 3010 Agronomy, Iowa State University, Ames, IA 50011. E-mail: panz@iastate.edu.

Abstract

We have run two regional climate models (RegCM2 and HIRHAM) forced by three sets of initial and boundary conditions to form a 2x3 suite of 10-year climate simulations for the continental U.S. at approximately 50 km horizontal resolution. The three sets of driving lateral boundary conditions are NCEP/NCAR reanalysis, a Hadley Centre coupled atmosphere-ocean GCM (HadCM2) simulation of contemporary climate, and a HadCM2 scenario of transient green house warming. Various biases are evaluated based the 2x3 experiment set, in addition to comparisons with a GCM simulation.

The reanalysis driven runs simulated reasonable precipitation climatology, which includes basic seasonality, overall precipitation distribution across the simulation domain, especially terrain induced orographic precipitation in the western mountains and along the Appalachians. The forcing bias (difference between GCM control driven and reanalysis driven runs) and inter-model bias are both largest in summer possibly due to the differing sub-grid scale processes in individual models. On the other hand, simulated change in precipitation is weakest in summer, posing a challenge for projecting future summer precipitation. The ratio of climate change to biases, which we use as one metric of confidence in projected climate changes, is substantially larger than 1 in several seasons and regions except in summer, when the ratios are always less than 1. The largest ratios are in California. Finally comparison of the RCM and GCM simulations shows that a sizable difference in precipitation magnitude exists between them with the RCMs generally closer to observations, potentially leaving room for RCMs to add value to GCM simulations.

1. Introduction

Over the past decade or so, there have been numerous modeling studies on global warming [e.g., *Gates 1992, Houghton et al. 1996*]. Public awareness of global-scale changes, such as global warming and environmental deterioration, has brought interest in projecting global changes onto local or regional scales where social and economic impacts may be evaluated. However, present-day computational resources needed for multi-decadal global change simulation limits the spatial resolution of global climate models (GCM) to scales (200-300km) larger than those needed for impacts analysis.

Early regional climate change studies focused on downscaling GCM projections to local scales of interest using statistical methods, which can be computationally inexpensive [e.g., *Karl et al 1990; Zorita et al. 1995*]. Dynamic downscaling by nesting a regional climate model (RCM) into a GCM was pioneered by *Dickinson et al. [1989]* and *Giorgi et al. [1992]* who first demonstrated its feasibility. Although computationally demanding, this approach has become a major tool in regional climate studies due to rapid advances in computer power and constant refinement in numerical techniques [e.g., *Cress et al. 1995, Jones et al. 1995, Podzun et al. 1995*, and *Christensen et al 1997,1998* for Europe; *Giorgi et al. 1994* and *Leung and Ghan 1999b* for North America; *McGregor and Walsh 1994* for Australia; *Semazzi et al. 1994* for Africa; and *Hirakuchi and Giorgi 1995*, and *Leung and Ghan 1999a* for Asia]. To our knowledge, the longest regional model simulations over the continental U.S. have been 3 years for analysis-driven simulations [*Giorgi et al. 1994, Giorgi and Shields 1999*] and 5 years for simulations driven by GCM output [*Giorgi et al. 1998*]. Somewhat longer simulations have been performed for sub-continental portions of the U.S. [e.g., *Leung and Ghan 1999b*].

Regional climate simulation is known to be model dependent, although for North America GCM simulations have shown less inter-model difference than most other regions of the world [*Houghton et al. 1996*]. *Machenhauer et al. [1998]* has reported the only published

multiple year intercomparison project that used regional models. These simulations covered a common area (Europe) and period, but the lateral boundary conditions, integration period, and simulation domain areas were only loosely controlled. The Project to Intercompare Regional Climate Simulations (PIRCS) has more strictly defined integration period and domain, but simulations to date have covered only 60 days [Takle *et al.* 1999].

In this study, we assess the accuracy of RCM precipitation simulations. Precipitation is an end product of many dynamic and thermodynamic processes in the atmosphere. For this reason, simulated precipitation climatology is quite likely to be model dependent, which weakens confidence in individual simulations of regional climate. However, precipitation strongly influences surface hydrology and energy budgets. Equally important, it is often a key variable for climate change impact assessments. Thus, there is great need to analyze from multiple perspectives the precipitation climatology simulated by RCMs and evaluate the uncertainties of these climatologies.

In the present report two regional climate models, RegCM2 [Giorgi *et al.*, 1993a, b] and the Danish Meteorological Institute's HIRHAM [Christensen *et al.*, 1996], have been used to produce suites of 10-year climate simulations for the continental U.S. at approximately 50 km horizontal resolution. Three sets of driving boundary conditions were used: NCEP/NCAR reanalysis, Hadley Centre coupled atmosphere-ocean GCM (HadCM2) output of contemporary climate, and a HadCM2 future scenario climate [Johns *et al.* 1997]. We use this suite of simulations to distinguish and compare a variety of biases affecting the accuracy of regional climate precipitation simulation:

- RCM (performance) bias - difference between reanalysis-driven RCM simulation and corresponding observations,
- forcing bias - difference between the GCM control climate driven and reanalysis driven runs,

- inter-model bias - difference between runs from different RCMs (HIRHAM minus RegCM2), both driven by reanalysis,
- G-R nesting bias – difference between the GCM run and RCM run driven by the GCM output, both for current climate.

Model (performance) bias depends on numerics, parameterization details, calibration choices, etc. of the individual models and measures model systematic errors and drift. Forcing bias measures how GCM imperfections in representing current climate affect the representation of regional climate by the RCM. Inter-model bias gives a range of RCM responses to external forcing, thereby indicating uncertainty in RCM downscaling. The G-R nesting bias (or more accurately difference) indicates the disagreement in results between the RCM and GCM. One of the most prominent model differences between a RCM and GCM is the horizontal resolution. The G-R nesting bias provides possible RCMs improvements over GCMs, primarily by higher resolution. Although we focus here on time-averaged precipitation, the methodology can be applied more broadly to analysis of other simulated fields.

Our intent here is not to analyze each of the biases in detail nor to search for causes. Rather, we present a methodology for identifying the most problematic biases that undermine confidence in climate change simulation. We also compare these precipitation biases with climate change, defined to be the difference between RCM runs driven by the GCM scenario and control simulations. This comparison helps us address the question of whether or not RCM downscaling provides meaningful changes in regional precipitation on scales important for climate impact studies

2. Model and Experiment Configuration

2. 1. RegCM2

RegCM2 [Giorgi *et al.*, 1993a, b] incorporates the CCM2 radiation package [Briegleb 1992] and the BATS version 1e [Dickinson *et al.* 1992] surface package. For this study, simulations used the modified Grell scheme [Grell 1993]. This mass flux scheme is a simplified version of Arakawa-Schubert convection [Arakawa and Schubert 1974] that assumes a single updraft and downdraft. Large-scale precipitation was computed using simple warm-cloud-physics, explicit-moisture scheme [Hsie *et al.* 1984]. The model has a single cloud-water predictive variable. The turbulence parameterization used Holtslag *et al.* [1990] non-local scheme that incorporates counter-gradient transport. The land surface scheme in RegCM2 has 18 categories of land use and 12 soil types. The model has two soil layers: top layer and root zone. The depth of the top layer is fixed at 10 cm while the root zone depth varies depending on land use type.

The model domain covers 101x75 grid points centered at (100°W, 37.5°N) with a horizontal resolution of 52 km (Fig. 1d). The model top is located at 100 hPa. The model in this study used 14 layers in the vertical, centered at $\sigma=0.995, 0.980, 0.950, 0.895, 0.815, 0.720, 0.615, 0.510, 0.405, 0.300, 0.210, 0.135, 0.070, \text{ and } 0.020$. Model lateral boundary conditions were assimilated by nudging in a buffer zone of 15 grid points [Davies and Turner 1977]. The simulation domain and buffer zone were chosen so that westerly flow enters far from high mountains, which can produce large interpolation errors [Hong and Juang 1998].

2. 2. HIRHAM

The HIRHAM model used in this study is based on the adiabatic part of the HIRLAM¹ short-range weather prediction model [Källén 1996]. Replacement of the standard HIRLAM physical parameterization package with that of the general circulation model ECHAM4 [Roeckner et al. 1996] has facilitated adaptation to long climate simulations [Christensen et al. 1996]. The resulting model, HIRHAM4, has been further documented in Christensen et al. [1998]. Sub-grid cumulus convection is parameterized by a mass flux scheme proposed by Tiedtke [1989]. In this scheme three types of convection - shallow, mid-level, and penetrative - are defined, each of which has different closure assumptions. Simulation of large-scale precipitation follows the formulation developed by Sundqvist [1978], in which fractional cloud cover is based on grid-scale moisture content. The scheme has a predictive variable (cloud water) for liquid phase while ice phase is diagnosed. The atmospheric radiation scheme is taken from ECMWF-model cycle 36 with addition of ozone, CFCs, and aerosols for climate simulations. The PBL scheme is based on a local K-type formulation. The land surface scheme uses 5 prognostic temperature layers and one (bucket) moisture layer. A zero flux lower boundary condition is applied for temperature. Runoff is calculated with the Arno scheme [Dümenil and Todini 1988], which softens the onset of runoff by introducing a distribution of soil water holding capacities in the grid box, depending on orographic slope. A simple one-layer snow model is coupled to the land surface scheme [DKRZ 1992; Christensen et al. 1996]. Lateral boundary conditions are assimilated through nudging within a 10-grid nudging zone. The discretization consists of 120x70 grid points with horizontal resolution of 0.5° and 19 vertical levels in sigma-pressure hybrid coordinates [Simmons and Burridge 1981] to the model top at 10 hPa.

¹ High Resolution Limited Area Model; developed by the national meteorological institutes in Denmark, Finland, Holland, Iceland, Ireland, Norway, and Sweden, and later in cooperation with France and Spain.

2. 3. Driving data and validating observations

Both observations and GCM output are used to drive the two RCMs. The observed forcing is obtained from the NCEP reanalysis [Kalnay *et al.*, 1996] augmented by AVHRR (Advanced Very high Resolution Radiometer) retrievals of sea surface temperature (SST) in the Gulf of California and buoy observations of surface temperature in the Great Lakes. The GCM output, both from contemporary and scenario runs, is taken from Hadley Centre GCM (Version 2) simulations [Johns *et al.* 1997], including SSTs.

Observed precipitation was obtained from the VEMAP (Vegetation/Ecosystem Modeling and Analysis Project) monthly precipitation archived on a 0.5°x0.5° grid. Our analysis is limited to the same region as the VEMAP archive, i.e., the continental U.S.

2. 4. Definitions of Experiments

Table 1 summarizes the main features of the comparisons. Both models are forced by the same output for identical periods. The models' domain sizes and resolution are based on the PIRCS North American grid [Takle *et al.*, 1999]. They differ slightly due to each model's horizontal coordinate system. Boundary conditions were updated every 6 hours within the buffer zone where the model-predicted variables were nudged to analyses or GCM output. All model runs were for 3 months plus 10 years, with the first 3 months discarded from analysis to reduce spinup effects.

Table 1. Description of experiments and forcing lateral boundary conditions

| | OBS-Driven | GCM-Control-Driven | GCM-Scenario-Driven |
|--------|-----------------------------|---|---|
| RegCM2 | NCEP reanalysis (1979-1988) | Hadley Centre GCM control run (around late1990's) | Hadley Centre transient GHG run (around 2050) |
| HIRHAM | NCEP reanalysis (1979-1988) | Hadley Centre GCM control run (around late1990's) | Hadley Centre transient GHG run (around 2050) |

OBS-Driven run. Boundary conditions for the observation-driven runs are from NCEP/NCAR reanalysis on a 28 σ -level, Gaussian grid (1.875° lat/lon). The simulation period (1979-1988) for the observation-driven runs coincides with AMIP experiments [Gates 1992].

GCM-Control-Driven run. The GCM driving data are from a HadCM2 contemporary (control) climate run. The HadCM2 is a finite-difference gridded model with horizontal resolution of 2.5° (lat) x 3.75° (lon) and 19 vertical levels. The 10-year window selected for present climate corresponds roughly to later years in the 20th century.

GCM-Scenario-Driven run. The HadCM2 driving output for our scenario runs is from a transient simulation that assumed a 1% per year increase rate of effective greenhouse gases. The time window corresponding to this run is around 2050. [It should be noted that aerosol effects are not included in this HadCM2 scenario run.] Detailed description of HadCM2 simulations appears in *Johns et al.* [1997].

Note that the reanalysis and the GCM contemporary climates are not for the same 10-year period. The OBS-driven simulation covers the specific years 1979-1988, whereas the HadCM2 GCM control run is not time specific, corresponding roughly to the late 20th century. To examine the importance of this difference in simulation periods, we have compiled a 40-year (1951-1990) precipitation climatology from the VEMAP archive and compared it with the 10-year average for our OBS-driven period (1978-1988). Differences between the two averages (not shown) are smaller than biases we discuss later, suggesting that our definition of forcing bias (GCM-control-driven minus OBS-driven) remains meaningful.

2. 5. Analysis Computations

All the biases (DP) are based on 10-yr averages over the complete annual cycle and over individual seasons: winter (Dec-Jan-Feb), spring (Mar-Apr-May), summer (Jun-Jul-Aug),

autumn (Sep-Oct-Nov). To account for spatial heterogeneity, biases are computed for specific regions (Fig. 1d). For example, RCM (performance) bias for a season in a region is given by

$$\Delta P_{RCM} = \frac{1}{N} \sum_{i=1}^N (P_i^m - P_i^o) \quad (1)$$

where P^o and P^m are seasonal mean of the variable in the region as observed and as simulated in the RCM, respectively, and N is the total number of grid points in the region. The other biases, ΔP_{RCM} , ΔP_{itmd} , ΔP_{GCM} , ΔP_{chng} , are similarly defined.

Regional bias measures the difference between two means but gives no information about spatial distribution. Two fields could have equal means but different spatial distribution. Thus, we compute also coefficients of spatial correlation between simulated and observed precipitation fields. For example, for RCM (performance) correlation,

$$r_{RCM} = \frac{\sum_{i=1}^N (P_i^o - \bar{P}^o)(P_i^m - \bar{P}^m)}{[\sum_{i=1}^N (P_i^o - \bar{P}^o)^2 \sum_{i=1}^N (P_i^m - \bar{P}^m)^2]^{1/2}} \quad (2)$$

where an overbar represents the regional average. Other coefficients, r_{forc} , r_{itmd} , r_{GCM} , r_{chng} , are evaluated similarly.

A potential advantage of RCMs over GCMs is that they can resolve spatial detail smoothed by a GCM's coarser resolution. We use the spatial standard deviation to analyze spatial variability of a variable and then compute the difference in spatial variability as

$$\Delta S_{RCM} = \left[\frac{\sum_{i=1}^N (P_i^o - \bar{P}^o)^2}{N-1} \right]^{1/2} - \left[\frac{\sum_{i=1}^N (P_i^m - \bar{P}^m)^2}{N-1} \right]^{1/2} \quad (3)$$

We compute ΔS_{forc} , ΔS_{itmd} , ΔS_{GCM} , ΔS_{chng} similarly.

3. Spatial and Seasonal Distribution of Biases

3. 1. RCM (Performance) Bias

The observed precipitation climatology (Fig. 1a) shows that the eastern U.S. is generally wet and the western U.S. is mostly dry but with heavy precipitation along the Pacific Northwest coast. Wetness in the lower Mississippi River basin comes largely from late summer/fall frontal systems. RegCM2 simulated the precipitation climatology reasonably well by capturing major characteristics, such as heavy amounts along the coasts, much less precipitation in the interior U.S., and the distinct east-west gradient (Fig. 1b). However, the model failed to capture the heavy rainfall in the lower Mississippi River basin, which appears to be caused by rainfall-producing systems not penetrating inland enough from the Gulf of Mexico. HIRHAM produced an annual precipitation climatology similar to RegCM2 and observations. Overall HIRHAM gave less precipitation than RegCM2 over most of the simulation domain except along the West Coast where HIRHAM's precipitation is 1-2 mm/d greater. HIRHAM's precipitation pattern agreed better with observations than RegCM2's over the lower Mississippi River basin. Both models captured quite well mountain precipitation such as Colorado upslope and California coastal rainfall as well as orographic precipitation over the Appalachian mountain range. Such small-scale orographic rainfall is a challenge to present-day GCMs because of their coarse resolution.

Precipitation across the continental U.S. has strong seasonal variations, so we break the analysis into seasons. For all seasons, RegCM2 tends to have a wet bias in the western U.S. and dry bias in the eastern U.S. (Fig. 2). In winter, the largest positive bias occurs over the Cascade Mountains in central WA and OR where it exceeds 2 mm/d. This bias could be due in part to the paucity of high-altitude observation stations [*Giorgi and Shields* 1999]. Bias magnitude in the central U.S. is less than 0.9 mm/d. The largest negative bias is along the Gulf coast. This may be due to the model's inability to resolve the local sea breeze, a major

contributor of rainfall along the coast. Spring bias has roughly the same overall pattern as winter.

The summer bias pattern is different from winter and spring. Biases are mostly within 0.3 mm/d. However, a negative bias center occurs in the Midwest with peak value exceeding -1.5 mm/d. The autumn bias distribution is similar to spring in the western U.S., but the biases in the eastern domain are quite different from other seasons, with a very strong negative bias region in the south-central U.S.

HIRHAM winter and spring biases (not shown) are very similar to those of RegCM2 except in summer, when negative bias occurs almost everywhere in the domain. The autumn bias in HIRHAM is smaller in magnitude both in the Pacific Northwest and the lower Mississippi basin.

3. 2. Forcing Bias

The forcing bias for RegCM2 is mostly positive; that is, the simulation driven by HadCM2 control climate gave larger rainfall amount than the reanalysis-driven simulation (Fig. 3). The bias pattern is quite similar for all seasons except for summer where a negative bias region occurred over the southwest U.S. Summer has largest forcing bias magnitude for most locations. A possible reason for this behavior is the predominance in summer of convective rainfall, which is difficult to simulate well. Fall has small forcing bias in most of the U.S. For all seasons the largest differences occur along the South and East coasts and to a lesser extent along the Pacific Northwest coast, possibly due to the coarse resolution of terrain and coastlines in the GCM (for example, the Florida peninsula does not exist in the HadCM2). HIRHAM's forcing bias is somewhat different from RegCM2's (not shown). The model has slightly negative values (0.3-0.9 mm/d) in the south-central U.S. It does not have a large positive bias along the South and East Coasts as found in RegCM2.

3. 3. Inter-Model Bias

RegCM2 has more rainfall than HIRHAM for the U.S. as a whole. There is strong regional variation in inter-model bias (Fig. 4). Inter-model bias (HIRHAM minus RegCM2) is negative in the west and positive in the east except for summer and along the East and West Coasts. For summer, RegCM2 simulated larger precipitation amounts than HIRHAM everywhere in the domain. The inter-model bias pattern is otherwise quite consistent in other seasons.

3. 4. G-R nesting Bias

The G-R nesting bias is the difference between precipitation from the HadCM2 control run itself and precipitation from the RCM run that is forced by the HadCM2 output. The G-R nesting bias is mostly negative across the domain (Fig. 5). Especially large negative bias occurs in the coastal western mountains in all seasons except summer, when the rainfall is small. G-R nesting biases are uniformly small in summer, in contrast to the forcing and inter-model biases. HIRHAM's pattern (not shown) is close to RegCM2 except in summer when the model has positive bias in west and east-central U.S.

Comparison with observations (Fig. 1a) shows that the HadCM2 simulation misses much of the orographic precipitation, which might be expected given the coarse resolution in HadCM2. The difference pattern corresponds well with terrain height. The larger error along the Gulf coast and eastern coast may be related to the coarse land-sea mask in the HadCM2.

3. 5. Climate Change

Simulated change in precipitation shows three distinct patterns: summer, winter, and transitional spring and fall (Fig. 6a). In winter, precipitation change is positive over the West Coast and the northeast states in agreement with *Giorgi et al.* [1994]. Precipitation increase exceeds 2 mm/d along the West Coast in winter, suggesting more frequent, more moist or

stronger winter storms over the eastern Pacific. Winter precipitation decreases along much of the Gulf of Mexico. The simulated precipitation change is small (± 0.5 mm/d) over the central U.S. HIRHAM simulated trends (not shown) are similar to RegCM2, but with weaker change along the West Coast.

Summer rainfall increase generally is small except for the south-central U.S. which has a 0.3-1.5 mm/d increase in precipitation. The relatively modest climate change projected for summer, contrasted with a relatively large inter-model bias during this season, reduces our confidence in summer regional precipitation estimates for future climates. Spring and fall changes are generally larger than summer and winter changes. Most of the large changes occur along coastal areas.

HIRHAM winter change is very similar to RegCM2 (Fig. 6b). Its spring change is weaker, especially in the eastern U.S., while the overall pattern is similar. Like RegCM2, its overall summer change is smallest, but its region of largest increase occurs farther east. The autumn changes are similar in magnitude between the two RCMs with HIRHAM's large wetting being more inland in the eastern U.S.

4. Regionalization of Biases and Correlation Analysis

4. 1. Seasonal Biases

To regionalize our analysis, we divide the continental U.S. into 5 regions (Fig. 1d) based on their climate characteristics, primarily following the Koeppen classification scheme [e.g., *Hidore and Oliver*, 1993]. The first region (Pacific Northwest coast) has a marine coastal climate. This region has a strong seasonal cycle in precipitation with a winter maximum. The second region (California) has a Mediterranean climate with dry summer and wet winter/spring. The third is the western mountain region with mostly dry climates. Here the precipitation climatology varies with local topography; most locations have a weak summer precipitation

maximum. The fourth (north-central U.S.) region has a cold continental climate while the fifth region (south-central U.S.) has hot and a humid climate.

Figure 7 summarizes RegCM2 biases and climate changes for each region and season from RegCM2 simulations. In the Pacific Northwest coast (region 1), the model performed well, and the annual model bias is only 0.3 mm/d, a combined result of negative values in winter and autumn and positive values in spring and summer. All RCM biases are small in summer and largest in winter, partly because of high precipitation in winter and low precipitation in summer. The forcing bias is quite consistent at around 0.2-1.0 mm/d in all seasons. G-R nesting biases are consistently negative and largest among all differences, including climate change, especially in winter when the bias magnitude reaches 2.5 mm/d. As discussed earlier, this appears to be due to better resolution of coastal topography in the RCM. Climate change is large and positive, except for summer when it is slightly negative. The largest increase is 2.5 mm/d in winter.

Relative biases (Table 2) allow us to compare more clearly regions with different annual rainfall totals. The relative RCM bias is normalized by the corresponding observation, whereas the relative forcing bias is normalized by the corresponding RegCM2 simulated value driven by observations, and so on (see Table 2). Relative biases are largest in summer and fall, but still only 12% (leftmost column in Table 2). Climate change ranges from -10% in summer to 36% in winter, with an annual mean of 24%.

In California (region 2) in winter, relative sizes of the biases are similar to those in region 1. In relative terms, the model bias has seasonal dependence; however, the high summer value of 217% can be traced to the very low (0.09 mm/d) summer precipitation in this region. The low precipitation could be in part attributable to the paucity of high altitude observation stations [*cf. Giorgi and Shields 1999*]. The relative forcing bias ranges from -12 to +14% although absolute values are small. The climate change ranges from -14% in summer to 69% in fall, with a change in annual mean of 56%. If we require relative climate change to be greater than the largest bias percentage of any bias in order to have confidence in climate change projection in

any given region, then annual average projections for California offer the most confidence, having climate changes that are nearly twice the highest model bias (56% vs. 30%). On a seasonal basis, winter, fall and spring all have relatively high confidence.

The mountain region (3) is characterized by changes that are small in absolute terms but large in relative terms. The changes are seasonally consistent (about 0.5-0.7 mm/d). The relative biases range from 31% in summer to 102% in winter with annual mean bias of 57%. The positive RCM bias (1 mm/d) and negative G-R nesting bias (-1.6 mm/d) in winter are the largest in this region. The model has an evident positive bias all year around. The forcing bias is very small, possibly because this region is far from the boundary zone so that differences in the driving lateral boundary conditions are minimized and the model internal dynamics predominate. The G-R nesting biases in this region (42% annually) are largest among all regions. This likely is due to the terrain difference between the RCM and GCM.

In the north-central U.S. (region 4), all absolute biases except the G-R nesting bias are small, as is climate change (within 0.4 mm/d). The results are characterized by large forcing biases in all seasons, varying model and inter-model biases and medium climate changes. In the south-central U.S. (region 5), the forcing and G-R nesting biases become larger than other biases, and climate change also is somewhat larger. The large biases appear to be associated with large differences in flow patterns over the Gulf of Mexico (not shown). If we use the confidence criterion described under region 1, the projected climate changes for spring in the north-central and south-central US have high confidence.

The forcing bias and G-R nesting bias always are negatively correlated, meaning that the RCM driven by GCM output has more precipitation compared to the reanalysis-driven run whereas the GCM itself gives noticeably less precipitation. The GCM appears less efficient in producing precipitation than the RCM when both are given similar larger-scale forcing [Jones *et al.* 1995].

In summary, we see: (1) Among all types of differences, including climate change, the G-R nesting bias is largest, reaching -2.5 mm/d in both the Pacific Northwest coast in winter (-37%) and south-central U.S. in summer (47%), compared to ± 1.0 mm/d in most other circumstances. (2) Among the 5 regions, the Pacific Northwest coast and south-central U.S. have largest RCM absolute bias, but relative RCM bias is largest in the mountain region (57%, annual), while biases are within $\pm 11\%$ in the other 4 regions. (3) Among the four seasons, summer has largest biases but smallest climate change, which lowers our confidence in summer climate projection. (4) Precipitation increase is simulated in most seasons and regions except for West Coast summer and East Coast winter; the ratio of climate change to various biases is highest along the West Coast, while the ratio is lowest in the southeast U.S. where precipitation is more convective and the unresolved sea-breeze circulation dominates along the coast.

HIRHAM climate change and G-R nesting biases (Fig. 8) in the Pacific coast (regions 1 and 2) are larger than RegCM2. Negative G-R nesting bias reaches -3.1 mm/d in winter. In region 2, climate changes are larger than other biases in all seasons (neglecting very dry summer) with maximum change of 3.6 mm/d in winter, the largest among all types of differences. HIRHAM, like RegCM2, has small biases and seasonal variations in regions 3 and 4. The largest difference between the two RCMs is in region 5 where biases and changes are smaller.

4. 2. Spatial Correlation and Standard Deviation

We calculate spatial correlation coefficients between fields used to compute each bias or change. Table 3 summarizes the correlation coefficients (r) for all regions and seasons. High correlation indicates smaller difference in spatial distribution of precipitation among the different simulations and observations. There is high correlation between the RegCM2 results for GCM control- and scenario-driven runs, with nearly all regions having $r > 0.94$. Thus even though

future precipitation increases, its overall spatial pattern remains relatively constant. This high correlation, of course, could be a model artifact since the two sets of model forcing conditions were generated by the same global model and the two simulations were carried out by the same regional model. The lowest correlation is between the modeled and observed precipitation, reflecting inherent challenges to numerical models to accurately simulate precipitation processes. The GCM-RCM correlations are generally low (except in region 2), a consequence of non-uniform G-R nesting bias in the south-central U.S. winter.

Among all regions, California has highest correlation ($r = 0.99$ for climate change and 0.55 for model performance). This extremely high correlation is the direct manifestation of orographic precipitation where resolving topography well is an important factor. By contrast, the lowest correlation is in the Pacific Northwest coast.

Spatial standard deviations in the reanalysis-driven run tend to be larger than observed in the West and smaller in the East (Table 4). The model's larger standard deviation in the West may be due in part to the tendency for observing stations to be located at lower elevations, whereas the model precipitation includes high and low elevation points. As expected spatial standard deviations in the RCM are larger than in the driving GCM, so that the GCM simulation is more spatially uniform than the RCM's. The RCM's future precipitation has more spatial uniformity in summer and stronger spatial heterogeneity in winter.

HIRHAM spatial correlation coefficients are generally larger than RegCM2's, especially in region 1, where HIRHAM's highest (0.85 , annual) and RegCM2's lowest (0.38) RCM correlations occur. The other types of correlations are comparable between the two models (not shown).

4. 3. Climate Change versus Biases

We computed the ratio of climate change to the largest in magnitude of RCM, forcing and inter-modal biases, for each region and season, i.e.,

$$R_{chg} = \frac{|\Delta P_{chg}|}{\text{Max} \{|\Delta P_{RCM}|, |\Delta P_{forc}|, |\Delta P_{itmd}|\}} \quad (4)$$

We did not include G-R nesting bias in (4) since it may represent an improvement rather than a deterioration in RCM simulation. Confidence in the simulated climate change increases as R_{chg} increases beyond 1. Conversely, we have less confidence in changes with $R_{chg} < 1$.

The climate change ratio is substantially larger than 1 in several seasons and regions (Fig. 9). We see that (1) summer R_{chg} are always less than 1; and (2) region 2 (California) has large R_{chg} . HIRHAM R_{chg} (Fig. 9) are similar to ReGCM2's. In regions 1 – 4, both models tend to have largest R_{chg} for the same seasons. This consistency between the models for large R_{chg} indicates that their range of climate change is meaningful for climate change impacts study.

We also counted the number of times a climate change magnitude for each season and region is greater than its corresponding magnitudes of RCM, forcing and inter-model biases (Fig. 10). Confidence in a change is greater for changes that exceed bias magnitudes most frequently. Especially noteworthy are seasons and regions where results from both models indicate high confidence in the simulated changes. Figure 10 shows that greatest confidence can be given to California change, which in both models exceeds all biases in all seasons except summer. The models indicate higher confidence in autumn changes for regions 1 and 4 and winter changes for the Pacific Northwest. Both models also indicate low confidence in summer change for all regions and low confidence any time of the year for changes in regions 3 and 5. Overall, the models' counts of change exceeding bias are within ± 1 of each other for every season and region (25 cases) except regions 1 and 5 in spring. The models thus demonstrate substantial consistency in the depiction of the confidence level of changes.

We close this section with a simple significance test. Using a T-test with 2x10 years of simulations, we examine the projected precipitation increases for statistical significance, given two means and variances. In most of the continental U.S., the T-value for annual mean precipitation exceeds 6 (not shown), which is much larger than the 95% confidence level, 1.73. RCM simulated climate change in annual precipitation is thus highly statistically significant. There are only two regions where the simulated precipitation increase is not statistically significant: areas in Texas and New Mexico and northern Minnesota, presumably the result of relatively weak precipitation increase.

5. Summary and Discussion

Regional climate model (RCM) simulation is relatively new compared to global climate model (GCM) simulation. Some aspects of RCM simulation are thus not as well tested as they have been for GCMs. For example, inter-model comparison among RCMs, although addressed in a few studies, has not been as extensive as for global models (e.g., Atmospheric Model Intercomparison Project; *Gates [1992]*). Furthermore RCM simulation is a lateral boundary problem, so that the quality of lateral boundary forcing plays an important role in RCM simulations. For example, present-day GCM output is often used to drive RCMs in regional climate simulations [e.g., *Giorgi et al. 1994*]. We must then establish how GCM-generated lateral forcing influences regional model results.

To address these issues, we have used two regional climate models (RegCM2 and HIRHAM) forced by three sets of lateral boundary conditions to produce six 10-year climate simulations for the continental U.S. at about 50-km horizontal resolution. Driven by common boundary conditions, the two models produced similar overall patterns in precipitation, although they differ in details of their spatial and seasonal distribution. Common precipitation climatology features simulated by both models include realistic orographic precipitation, east-west gradients, and reasonable annual cycles over different geographic locations. On the other hand, both

models miss heavy precipitation in the lower Mississippi River basin. (In an experiment where a larger group of RCMs simulated a 2-month period, almost all models had difficulty in capturing heavy rainfall in the lower Mississippi River basin; *Takle et al.* [1999].) A possible cause for this error is insufficient moisture transport so that rainfall did not penetrate inland enough from the Gulf of Mexico.

Spatial correlation coefficients of precipitation have been computed between simulation pairs in the 2x3 set. The climate change correlation is highest and the RCM performance correlation is lowest while forcing and inter-model correlations are of intermediate size. The high climate change correlation suggests that even though future precipitation increases, its overall spatial pattern remains relatively constant. The low RCM performance correlation shows a modeling challenge to reproduce observed spatial precipitation patterns.

Projected precipitation changes are positive over most areas during all seasons except winter near the Texas coast. The annual relative increase is 15-55% depending on the region. The dry west has larger increases than the wet east in both relative and absolute changes. While agreeing with typical GCM simulations in terms of general distribution and seasonality, the RCMs examined here provide more spatial variability, especially in mountainous areas. Comparison of the RCM and GCM simulations shows that a sizable difference in precipitation magnitude exists between them, potentially leaving room for RCMs to add value to GCM simulations.

The bias analysis shows shown that (1) climate change is a couple of times larger than the combined biases in most reasons and regions; (2) summer ratios are always less than 1; and (3) the ratio of climate change to bias is especially large in the California region. Finally, the comparison of the RCM and GCM simulations showed that a sizable difference exists between them with the RCMs generally closer to observations, potentially leaving room for RCMs to add value to GCM simulations.

The bias comparisons indicate where improvements in modeling or understanding of model behavior are most needed in order to improve confidence in climate change projections. For example, forcing bias is large for all seasons in the southeastern U.S. Since the RCM (performance) bias for this region is relatively small, reducing forcing bias requires improved contemporary climate GCM simulation for the southeastern U.S. For the two regions along the West Coast, inter-model bias is relatively large, implying that improvements in RCM modeling are important for increasing confidence as well as consistency in projected climate change. The West Coast inter-model differences are largest in winter, suggesting that RCM interaction between onshore flow and topography needs improvement. Finally, one of the consistently largest biases is the G-R nesting bias. As noted earlier, this bias does not necessarily imply error in regional precipitation simulation. For example, the better resolution of topography by the RCM compared to the GCM may mean that the RCM is simulating topographic precipitation more accurately, so that the bias represents an improvement in regional precipitation simulation. The relatively small RCM (performance) bias compared to G-R nesting bias in the Pacific Northwest is a case in point.

Acknowledgements

The computer resources used for the RegCM2 simulations in this study were provided by NCAR CSL facility. The computer resources used for HIRHAM are provided by the Danish Meteorological Institute. The Electric Power Research Institute, California Energy Commission and U.S. National Oceanic and Atmospheric Administration [grant NA86GP0572] provided financial support for this project. We are grateful to Filippo Giorgi and Christine Shields for providing consulting on RegCM2, and David Hassell and Richard Jones of the Hadley Centre, who kindly provided HadCM2 outputs. We also

thank Philippe Lopez for assistance on setting up and running the HIRHAM model for the US domain.

References

- Arakawa, A, and W.H. Schubert, Interaction of a cumulus cloud ensemble with the large-scale environment, Part I. *J. Atmos. Sci.*, 31, 674-701, 1974.
- Briegleb, B. P., Delta-Eddington approximation for solar radiation in the NCAR community climate model, *J. Geophys. Res.*, 97, 7603-7612, 1992.
- Christensen, J.H., O. B. Christensen, P. Lopez, E. van Meijgaard, and M. Botzet, The HIRHAM4 Regional Atmospheric Climate Model; *DMI Scientific Report 96-4*, 1996 [Available from DMI, Lyngbyvej 100, Copenhagen Ø, Denmark].
- Christensen, J. H., B. Machenhauer, R. G. Jones, C. Schär, P. M. Ruti, M. Castro, and G. Visconti, Validation of present-day regional climate simulations over Europe: LAM simulations with observed boundary conditions. *Climate Dyn.*, 13, 489-506, 1997.
- Christensen O.B., J.H. Christensen, B. Machenhauer and M. Botzet, Very high-resolution regional climate simulations over Scandinavia – Present climate, *J. Clim.*, 11, 3204-3229, 1998.
- Cress, A., D. Majewski, D. R. Podzun, and V. Renner, Simulation of European climate with a limited area model. Part I: Observed boundary conditions. *Beitr. Phys. Atmos.*, 68, 161-177, 1995.
- Davies, H. C., and R. E. Turner, Updating prediction models by dynamic relaxation: An examination of the technique. *Quart. J. Roy. Meteor. Soc.*, 103, 225-245, 1977.
- Dickinson, R. E., R. M. Errico, F. Giorgi, and Bates, A regional climate model for the western United States. *Climate Change*, 12, 383, 1989.

- Dickinson, R. E., A. Henderson-Sellers, and P. J. Kennedy, Biosphere-atmosphere transfer scheme (BATS) version 1e as coupled to NCAR community climate model, *NCAR Tech. Note 387+STR*, 72 pp., 1992 [Available from Natl. Cent. for Atmos. Res., Boulder, Colo.].
- DKRZ, The ECHAM-3 atmospheric general circulation model, DKRZ Tech. Rep. No. 6, 186pp., Hamburg, 1992.
- Dümenil, L., and E. Todini, A rainfall-runoff scheme for use in the Hamburg climate model. *Advances in the theoretical hydrology*, Vol. 1, EGS Series of Hydrological Sciences, Elsevier, 129-157, 1988.
- Gates, W. L., The Atmospheric Model Intercompression Project. *Bull. Amer. Meteor. Soc.*, 73, 1962-70, 1992.
- Giorgi, F., M.R. Marinucci, and G. Visconti, A 2xCO₂ climate change scenario over Europe generated using a Limited Area Model nested in a General Circulation Model. II: Climate change scenario. *J Geophys. Res.*, 97, 10011-10028, 1992.
- Giorgi, F., M. R. Marinucci, G. T. Bates, and G. De Canio, Development of a second-generation regional climate model (RegCM2), I, Boundary-layer and radiative transfer, *Mon. Wea. Rev.*, 121, 2794-2813, 1993a.
- Giorgi, F., M. R. Marinucci, G. T. Bates, and G. De Canio, Development of a second-generation regional climate model (RegCM2). Part II: convective processes and assimilation of lateral boundary conditions. *Mon. Wea. Rev.*, 121, 2814-2832, 1993b.
- Giorgi, F., and L. O. Mearns, Approaches to the simulation of regional climate: A review. *Rev. of Geophysics*, 29, 191-216, 1991.
- Giorgi, F, L.O., Mearns, C. Shields and L. McDaniel, Regional nested model simulations of present day and 2xCO₂ climate over the Central Plains of the U.S., *Climate Change*, 40, 457-493. 1998.

- Giorgi, F. and C. Shields, Tests of precipitation parameterizations available in the latest version of the NCAR regional climate model (RegCM) over the continental U.S., *J. Geophys. Res.*, *104*, 6353-6376, 1999.
- Giorgi, F., C. Shields, and G. T. Bates, Regional climate change scenario over the United States produced with a nested regional climate model. *J. Climate*, *7*, 375-399, 1994.
- Grell, G. A., Prognostic evaluation of assumptions used by cumulus parameterizations, *Mon. Wea. Rev.*, *121*, 764-787, 1993.
- Hidore, J.J., and J.E. Oliver, *Climatology - An Atmospheric Science*, Macmillan Publishing Company, New York, New York. 1993.
- Hirakuchi, H, and F. Girogi, Multi-year present day and 2xCO₂ simulations of monsoon climate over Asian and Japan with a regional climate model nested in a general circulation model, *J. Geophys. Res.*, *100*, 21105-21126. 1995.
- Houghton J.T., L.G. Meria Fiho, B.A. Callander, N. Harris, A. Kattenberg, and Maskell, *Climate change 1995 -- The science of climate change*. (Eds). Cambridge University Press, 572pp, 1996.
- Holtslag, A.A.M., E.I.F., de Bruijn, and H.L. Pan, A high resolution air mass transformation model for short-range weather forecast, *Mon. Wea. Rev.*, *118*, 1561-1575, 1990.
- Hong, S.-Y., and H.-M. H. Juang, Orography blending in the lateral boundary condition of a regional model, *Mon. Wea. Rev.*, *126*, 1714-1718.
- Hsie, E.-Y., R. A. Anthes, and D. Keyser, Simulations of frontogenesis in a moist atmosphere using alternative parameterizations of condensation and precipitation. *J. Atmos. Sci.*, *41*, 2701-2716, 1984
- Jones, R. G., J. M. Murphy, and M. Noguer, Simulation of climate change over Europe using a nested regional-climate model. I: Assessment of control climate,

- including sensitivity to location of boundaries. *Qurt. J. Roy. Meteor. Soc.*, 121, 1413-1450, 1995.
- Johns, T. C., R. E., Carnell, J. F., Crossley, J. M. Gregory, J. F. B. Mitchell, C. A. Senior, S. F. B. Tett, and R. A. Wood, The second Hadley Centre coupled ocean-atmosphere GCM: model description, spinup, and validation. *Climate Dyn.*, 13, 103-134, 1997.
- Källén, E., 1996: HIRLAM documentation manual, system 2.5. Swedish Meteorological and Hydrological Institute, (Eds), 126 pp. 1996 [Available form SMHI, S-60176 Norrköping, Sweden].
- Kalnay, E., and co-authors, The NCEP/NCAR 40-Year Reanalysis Project, *Bull. Amer. Meteor. Soc.*, 77, 437-471, 1996.
- Karl, T.R., W.-C. Wang, M.E. Schemminger, and R.W. Knight, A method of relating general circulation simulated climate to the observed local climate, Part I: Seasonal statistics., *J. Climate*, 3, 1053-1079, 1990.
- Leung, L.R., S.J., Ghan, Z.-C. Zhao, Y. Luo, W.-C., Wang, and H.-L., Wei, Intercomparison of regional climate simulations of the 1991 summer monsoon in eastern Asia, *J. Geophys. Res.*, 104, 6425-6554, 1999a.
- Leung, L.R., and S.J. Ghan, Pacific Northwest climate sensitivity simulated by a regional climate model driven by a GCM. Part I: Control simulations, *J. Climate* (in press), 1999b.
- Machenhauer B., M. Windelband, M. Botzet, J.H. Christensen, M. Déqué, R.G. Jones, P.M. Ruti and G. Visconti, 1998: Validation and analysis of regional present-day climate and climate simulations over Europe. *MPI Report No. 275*, Max-Planck-Institute, Hamburg.
- McGregor, J. L., and K. Walsh, Climate change simulations of Tasmanian precipitation using multiple nesting. *J. Geophys. Res.*, 99, 20889-20905, 1994.

- Podzun, R., C. D. Majewski, and V. Renner, Simulation of European climate with a limited area model. Part I: A GCM boundary conditions. *Beitr. Phys. Atmos.*, 68, 178-225, 1995.
- Roeckner, E. and Coauthors, The atmospheric general circulation model ECHAM-4: Model description and simulation of present-day climate. MPI Rep. 218, Max-Planck-Institute, Hamburg, 1996.
- Semazzi, F.H.M, N-H. Lin, Y.-L. Lin, and F. Giorgi, A nested model study of the Sahelian climate response to sea surface temperature anomalies. *Geophys. Res. Lett.*, 20, 2897-2900, 1994.
- Simmons, A., and D.M. Burridge, An energy and angular momentum conserving vertical finite difference scheme and hybrid vertical coordinates. *Mon. Wea. Rev.* 109, 758-766, 1981.
- Small, E.E, F. Giorgi, and L. C. Sloan, Regional climate model simulation of precipitation in central Asia: Mean and interannual variability, *J. Geophys. Res.*, 104, 6563-6602, 1999.
- Sundqvist, H., A parameterization scheme for non-convective condensation including prediction of cloud water content. *Quart. J. Roy Meteor. Soc.*, 104, 677-690, 1978.
- Takle, E.S., W.J. Gutowski, Jr., R.W. Arritt, Z. Pan, C.J. Anderson, R. Silva, D. Caya, S.-C. Chen, J.H. Christensen, S.-Y. Hong, H.-M. H. Juang, J.J. Katzfey, W.M. Lapenta, R. Laprise, P. Lopez, J. McGregor and J.O. Roads, Project to Intercompare Regional Climate Simulations (PIRCS): Description and initial results. *J. Geophys. Res.*, 104, 19443,19461, 1999.
- Tiedtke, M., 1989, A comprehensive mass flux scheme of cumulus parameterization in large-scale models. *Mon. Wea. Rev.*, 117, 1179-1800.

Zortea, E, J.P., Hughes, D.P., Lettenmaier, and H. von Storch, Stochastic characterization of regional circulation patterns for climate model diagnosis and estimation of local precipitation. *J. Climate*, 8, 1023-1042, 1995.

List of Figures

- Fig.1. Ten-year (1979-188) annual precipitation (mm): (a) observed from VEMAP (Vegetation/Ecosystem Modeling and Analyses Project), (b) simulated by RegCM2, and (c) simulated by HIRHAM, and (d) boundaries of regions (see text for detail).
- Fig. 2. Seasonal breakdown of RCM bias (reanalysis-driven simulation – observation) for precipitation (mm/d) averaged the 10 years.
- Fig. 3. As Fig. 2, but for forcing bias (GCM current-climate-driven run – reanalysis-driven run).
- Fig. 4. As Fig. 2, but for inter-model bias (HIRHAM RCM run – RegCM2 run, both driven by reanalysis).
- Fig. 5. As Fig. 2, but for G-R nesting bias (GCM's control run – RCM run driven by GCM's control run).
- Fig. 6. As Fig. 2, but for climate change (GCM scenario climate driven run – GCM current climate driven run): (a) RegCM2 and (b) HIRHAM.
- Fig. 7. Comparisons of various biases with climate change in seasonal precipitation in different regions (RegCM2).
- Fig. 8. As Fig. 7 but for HIRHAM.
- Fig. 9. The climate change ratio (change divided by maximum bias) in different seasons and regions
- Fig. 10. Number counts when the climate change is greater than any of RCM bias, forcing bias or inter-model bias.

| Table 2. Relative biases and climate change in precipitation (%) for RegCM2 | | | | | |
|--|------------|------------|------------|------------|------------|
| RCM bias (% observation) | | | | | |
| region | 1 | 2 | 3 | 4 | 5 |
| win | -9 | -14 | 102 | 50 | -14 |
| spr | 3 | 0 | 46 | 21 | -6 |
| sum | 12 | 217 | 30 | -4 | 14 |
| aut | -12 | -5 | 56 | 0 | -21 |
| ann | -6 | -6 | 57 | 11 | -6 |
| Forcing bias (% of reanalysis driven) | | | | | |
| region | 1 | 2 | 3 | 4 | 5 |
| win | 14 | 11 | 11 | 21 | 51 |
| spr | 20 | 2 | 2 | 7 | 29 |
| sum | 19 | 14 | 6 | 19 | 34 |
| aut | 24 | -12 | 0 | 6 | 36 |
| ann | 18 | 4 | 5 | 13 | 37 |
| Inter-model bias (% of RegCM2) | | | | | |
| region | 1 | 2 | 3 | 4 | 5 |
| win | 19 | 32 | -16 | 13 | 10 |
| spr | 13 | 21 | -16 | 0 | -4 |
| sum | -10 | -57 | -89 | -37 | -64 |
| aut | 23 | 19 | -38 | -4 | -4 |
| ann | 16 | 24 | -34 | -7 | -17 |
| G-R nesting bias (% of RCM run) | | | | | |
| region | 1 | 2 | 3 | 4 | 5 |
| win | -37 | -23 | -67 | -54 | -32 |
| spr | -37 | -35 | -38 | -16 | -16 |
| sum | -42 | -60 | -10 | -21 | -47 |
| aut | -39 | -35 | -44 | -41 | -45 |
| ann | -38 | -30 | -42 | -31 | -35 |
| Climate change (% of current) | | | | | |
| region | 1 | 2 | 3 | 4 | 5 |
| win | 36 | 60 | 30 | 17 | -4 |
| spr | 17 | 48 | 29 | 25 | 29 |
| sum | -10 | -14 | 6 | 1 | 9 |
| aut | 23 | 69 | 27 | 17 | 27 |
| ann | 24 | 56 | 23 | 14 | 15 |

| Table 3. Correlation coefficients in precipitation | | | | | |
|--|-------------|-------------|-------------|-------------|-------------|
| for RegCM2 | | | | | |
| RCM bias | | | | | |
| region | 1 | 2 | 3 | 4 | 5 |
| win | 0.39 | 0.51 | 0.7 | 0.94 | 0.65 |
| spr | 0.34 | 0.55 | 0.73 | 0.85 | 0.41 |
| sum | 0.57 | 0.78 | 0.8 | 0.41 | 0.69 |
| aut | 0.48 | 0.56 | 0.58 | 0.84 | 0.24 |
| ann | 0.38 | 0.55 | 0.65 | 0.87 | 0.59 |
| Forcing bias | | | | | |
| region | 1 | 2 | 3 | 4 | 5 |
| win | 0.93 | 0.98 | 0.97 | 0.99 | 0.72 |
| spr | 0.93 | 0.99 | 0.94 | 0.93 | 0.3 |
| sum | 0.96 | 0.98 | 0.7 | 0.86 | 0.87 |
| aut | 0.93 | 0.99 | 0.96 | 0.87 | 0.91 |
| ann | 0.95 | 0.99 | 0.96 | 0.96 | 0.85 |
| Inter-model bias | | | | | |
| region | 1 | 2 | 3 | 4 | 5 |
| win | 0.5 | 0.92 | 0.91 | 0.88 | 0.85 |
| spr | 0.53 | 0.95 | 0.85 | 0.89 | 0.67 |
| sum | 0.69 | -0.07 | 0.62 | 0.85 | 0.81 |
| aut | 0.62 | 0.85 | 0.88 | 0.92 | 0.68 |
| ann | 0.49 | 0.9 | 0.88 | 0.92 | 0.74 |
| G-R nesting bias | | | | | |
| region | 1 | 2 | 3 | 4 | 5 |
| win | 0.49 | 0.8 | 0.66 | 0.82 | 0.81 |
| spr | 0.58 | 0.88 | 0.77 | 0.58 | 0.05 |
| sum | 0.75 | 0.82 | 0.85 | 0.32 | 0.31 |
| aut | 0.73 | 0.93 | 0.69 | 0.72 | 0.54 |
| ann | 0.52 | 0.88 | 0.7 | 0.61 | 0.39 |
| Climate change | | | | | |
| region | 1 | 2 | 3 | 4 | 5 |
| win | 0.81 | 0.99 | 0.97 | 0.99 | 0.87 |
| spr | 0.76 | 0.99 | 0.88 | 0.89 | 0.9 |
| sum | 0.96 | 0.99 | 0.96 | 0.79 | 0.97 |
| aut | 0.91 | 0.99 | 0.97 | 0.98 | 0.96 |
| ann | 0.85 | 0.99 | 0.94 | 0.97 | 0.99 |

| Table 4. Standard deviation biases in precipitation (mm) | | | | | |
|--|--------------|------------------|--------------|--------------|--------------|
| between different simulations for RegCM2 | | | | | |
| | | | | | |
| | | RCM bias | | | |
| region | 1 | 2 | 3 | 4 | 5 |
| win | 2.62 | 0.99 | -0.27 | -0.13 | 0.3 |
| spr | 1.26 | 0.24 | 0.05 | -0.01 | 0.2 |
| sum | 0.04 | -0.11 | 0.02 | -0.26 | -0.28 |
| aut | 1.6 | 0.48 | -0.08 | 0.04 | -0.22 |
| ann | 1.41 | 0.41 | -0.05 | -0.14 | -0.04 |
| | | | | | |
| | | Forcing bias | | | |
| region | 1 | 2 | 3 | 4 | 5 |
| win | 0.02 | 0.17 | 0.01 | 0.22 | 0.75 |
| spr | 0.18 | 0.13 | 0.07 | 0.11 | 0.43 |
| sum | 0.03 | 0.1 | 0.22 | 0.04 | 1.14 |
| aut | 0.48 | 0.01 | 0.24 | 0.37 | 1.25 |
| ann | 0.15 | 0.1 | 0.11 | 0.18 | 0.92 |
| | | | | | |
| | | Inter-model bias | | | |
| region | 1 | 2 | 3 | 4 | 5 |
| win | 1.45 | 0.45 | 0 | -0.15 | -0.03 |
| spr | 0.57 | 0.07 | 0.14 | -0.19 | 0.3 |
| sum | 0.06 | -0.08 | -0.27 | -0.21 | -0.77 |
| aut | 0.89 | 0.28 | 0.1 | 0.02 | -0.37 |
| ann | 0.74 | 0.16 | 0.1 | -0.12 | -0.19 |
| | | | | | |
| | | G-R nesting bias | | | |
| region | 1 | 2 | 3 | 4 | 5 |
| win | 0.33 | -0.35 | -0.31 | -0.49 | -0.74 |
| spr | -0.12 | -0.22 | -0.09 | -0.04 | -0.09 |
| sum | -0.11 | -0.14 | 0.04 | -0.03 | -1.5 |
| aut | -0.3 | -0.15 | -0.26 | -0.44 | -1.58 |
| ann | -0.13 | -0.22 | -0.21 | -0.3 | -1.13 |
| | | | | | |
| | | Climate change | | | |
| region | 1 | 2 | 3 | 4 | 5 |
| win | 0.4 | 0.43 | 0.59 | 0.38 | 0.01 |
| spr | -0.02 | 0.21 | 0.14 | 0.2 | 0.48 |
| sum | 0.06 | -0.09 | -0.07 | -0.08 | -0.04 |
| aut | -0.25 | 0.33 | 0.19 | -0.05 | 0.2 |
| ann | -0.05 | 0.22 | 0.17 | 0.08 | 0.16 |

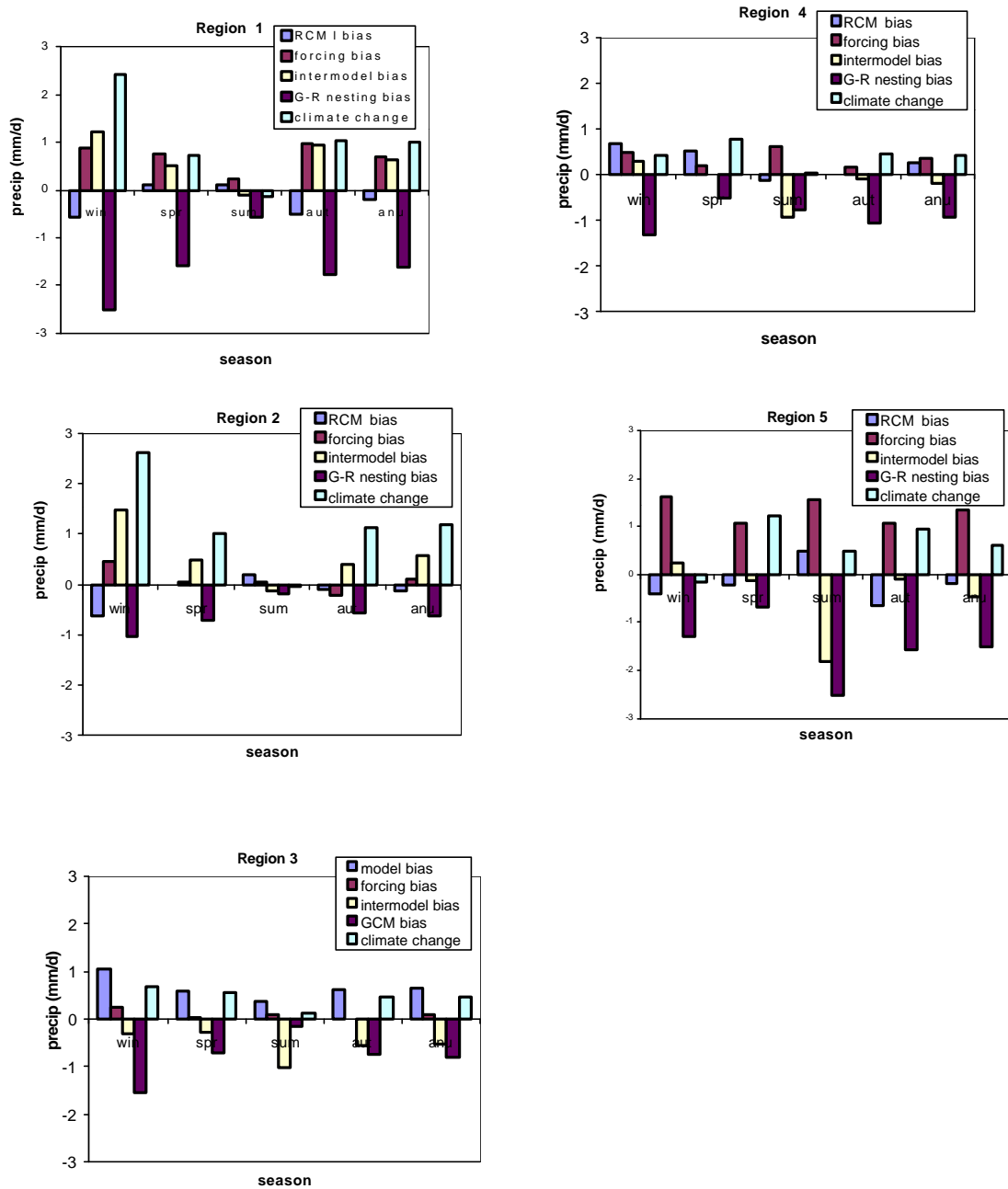


Fig. 7. Comparisons of various biases with climate change in seasonal precipitation in different regions (RegCM2).

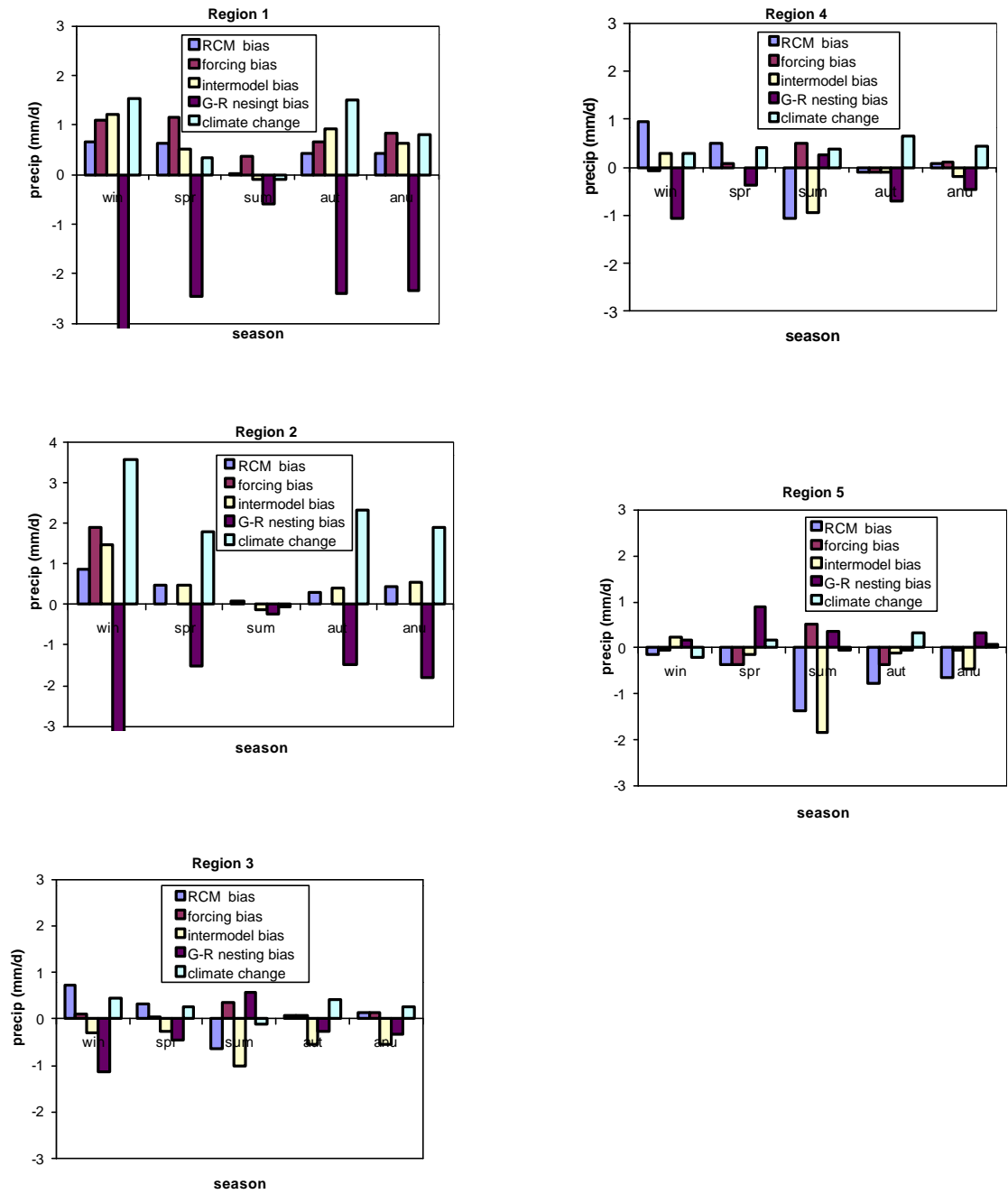


Fig. 8. As Fig. 7 but for HIRHAM.

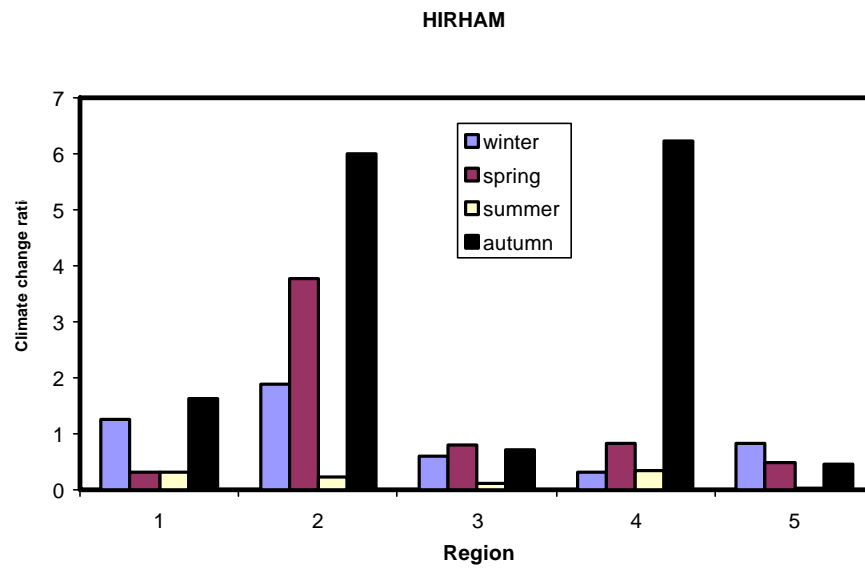
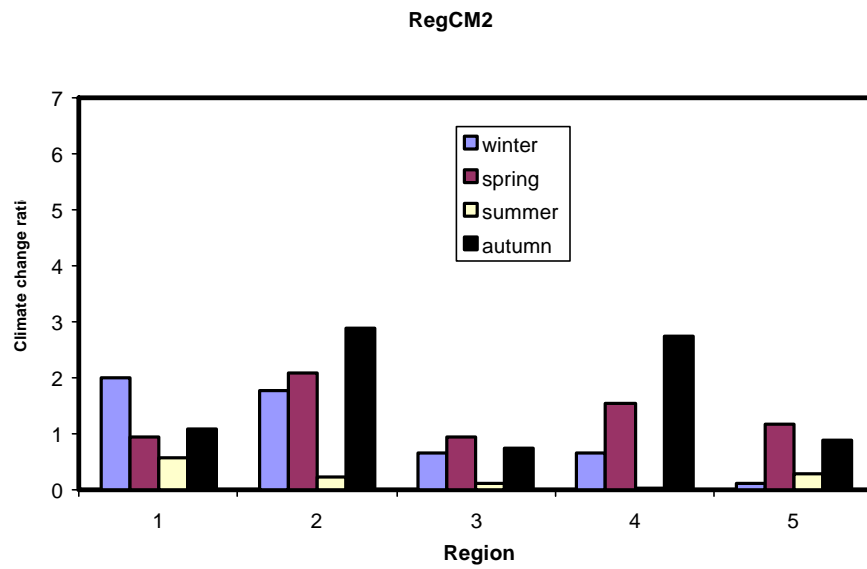


Fig. 9. The climate change ratio (change divided by maximum bias) in different seasons and regions

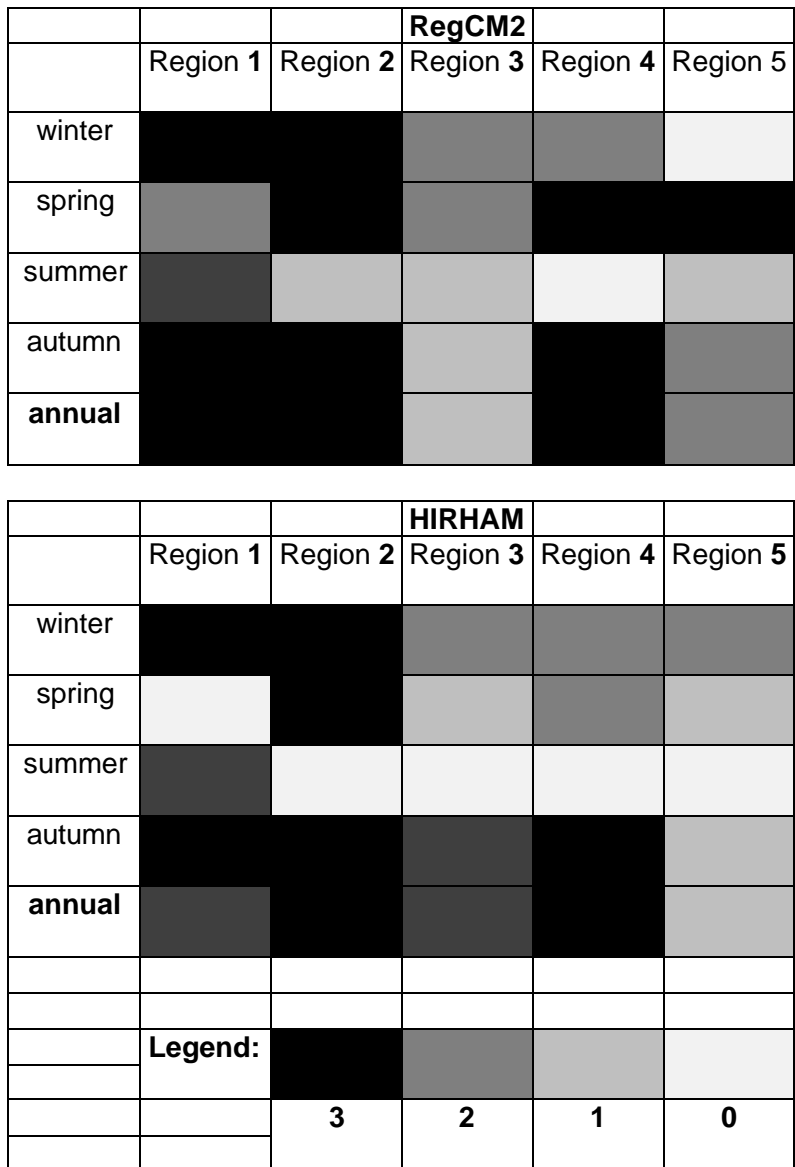


Fig. 10. Number counts when climate change is greater than any of RCM bias forcing bias or inter-model bias.